Ab initio study of Ti–C precipitates in hcp titanium: Formation energies, elastic moduli and theoretical diffraction patterns

D.A. Aksyonov*, A.G. Lipnitskii, Yu.R. Kolobov

The Center of Nanostructured Materials and Nanotechnologies, Belgorod State University, Belgorod, Russian Federation

ABSTRACT

The Ti–C system is poorly studied at low carbon concentrations (<1 at.%). This region is important because Ti–C dispersed phases can improve thermal stability of commercially pure nanostructured α-Ti alloys. We developed based on first principles new method which allows to predict formation of precipitates at low concentrations of impurities in metallic matrix. Using this method probabilities of formation of Ti–C phases in α-Ti were computed. It was found that most favourable phases at 200–800 K are Ti_2C and Ti_3C_2. Elastic moduli and diffraction patterns of most favourable Ti–C phases are also presented.
© 2012 Elsevier B.V. All rights reserved.

1. Introduction

Dispersions of fine particles such as precipitates can be very effective for strengthening and improving the thermal stability of nanostructured materials [1,2], which are attractive due to high flow stress combined with sufficient ductility. Possible example of such material is intensively studied commercially pure nanostructured α-titanium (CP-nTi) [3] which has high biocompatibility [4] and superior strength [5] in comparison to coarse-grained Ti.

Several experimental works [6–8] confirmed high thermal stability of CP-nTi up to 723 K while recent theoretical investigations [8] showed rapid transition of very pure nTi in coarse-grained state even at room temperatures. This is in agreement with low thermal stability of pure nanostructured metals [9]. Hence there are some mechanisms of grain boundary pinning in CP-nTi and one of them is precipitation of secondary phases from existing impurities. Total atomic percentage of impurities in CP-nTi (Grade-4 alloy) is about 3 at.% and may be enough for decrease of grain growth. It is known [10] that microstructure stabilization in polycrystal with the most probable grain size 20 nm could be achieved at the particle volume fraction of the order of 0.001. For example, precipitation of 2.6 at.% of Mg and Zr sufficiently increases thermal stability of Al matrix [11]. Investigation of thermal stability mechanisms in CP-nTi is very important because this material is used in lifetime dental implants production [4] and need technologically necessary heat treatment [12].

There are several experimental studies of CP-nTi in which Ti–C particles were observed. For example coherent Ti–C particles in nTi have been observed in Ref. [13]. Bushnev et al. [13] propose existence of particles with Ti_2C stoichiometry, while in Ref. [14] have been observed only TiC particles. Semenova et al. [15] have not observed particles but found increased concentration of C, N, and O at grain boundaries in nTi Grade 4. Finally there is work in which CP Ti was doped with additional C and Si atoms. As result formation of Ti–C, Ti–Si precipitates and increase of nTi thermal stability is noted [16]. Nevertheless information about crystal structure of particles which determine interaction with grain boundaries is incomplete and in some cases absent. Small sizes of particles and their metastable character is the main restriction for their experimental investigation. It is known from expended review of Ti–C system [17] there are different possibilities for crystal structure of Ti–C particles. Nevertheless Ti–C system is well studied and established experimentally, quite different ordering temperatures and concentration ranges of existence have been reported; see Table 1. The most recent Ti–C phase diagrams [18] contain many of Ti–C structures, but in all cases there is no information about dispersed phases (precipitates) in low concentration carbon region.

Absence of information about structure of Ti–C precipitates in dependence from temperature is the hindering factor for thermal stability investigation of α-Ti alloys. The mechanical properties of Ti–C precipitates which has influence on matrix properties is also unknown. However, lack of information about structure and mechanical properties of Ti–C particles can be eliminated with the use of computer simulation methods.

In present work we provide a new approach for calculating specific formation energies of phases in matrix material accounting

Table 1
Experimental highest temperatures (T) of existence, ranges of existence and diffraction reflexes of Ti–C phases.

Phase	Source	Highest T of existence (K)	Ranges of existence	Specific diffraction reflexes
Ti_2C (227)	Ref. [22]	<2173	$TiC_{0.52-0.71}$	(1/2 1/2 1/2), (3/2 1/2 1/2), (3/2 3/2 1/2), (3/2 3/2 3/2)
	Ref. [23]	970–1010	$TiC_{0.49-0.59}$	
	Ref. [24]	770–790	$TiC_{0.59}$; $TiC_{0.62}$	
	Ref. [25][a]	<1773	–	
Ti_2C (166)	Ref. [23]	940–980	$TiC_{0.55-0.59}$	(1/2 1/2 1/2), (3/2 1/2 1/2), (3/2 3/2 3/2)
	Ref. [26]	anneling 1053–1023	$TiC_{0.625}$	
	Ref. [27]	970	$TiC_{0.59}$	
	Ref. [28]	<1053	$TiC_{0.62}$	
	Ref. [24]	<770	$TiC_{0.59}$; $TiC_{0.62}$	
Ti_3C_2 (20)	Ref. [29]	873	$TiC_{0.64-0.68}$	(2/3 2/3 0), (1/3 −2/3 −1/2), (−1/3 2/3 −1/2), (5/8 5/8 0)
	Ref. [23]	980–1000	$TiC_{0.62-0.68}$	

[a] Ti_2C phase on Ti–6%Al–4%V/TiC interface.

underling physics. Using this approach we report energetically favourable Ti–C phases in α-Ti and their structures obtained by *ab initio* PAW GGA plane-waved method. On the base of phases we propose possible crystalline structures of Ti–C precipitates. Using formation energies of Ti–C phases in α-Ti and the law of mass action [19] we developed method for calculation of impurities distribution by different energetic states in dependence of temperature and found carbon distribution by several most favourable Ti–C structures up to temperature of α-Ti to β-Ti polymorphic transformation. To predict mechanical properties of Ti–C particles and their influence on Ti matrix we calculated elastic moduli of most favourable Ti–C phases. Also we provide calculated theoretical diffraction patterns of Ti–C phases that can be used for interpretation of present and future experimental investigations. It must be mentioned that nevertheless there are many works on Ti–C system, such methodology of consideration of Ti–C phases in hcp titanium is made for the first time and can be used for other impurities in many metallic matrices. The results may be used for further investigation of nTi thermostability.

2. Methodology

Despite the very attractive possibility of grain boundary engineering with dispersed particles, there are few examples of such specially engineered materials [1]. The main reasons are absence of information about dispersive metastable phases in phase diagrams and robust methods for prediction of structure of dispersed particles. Below we describe quiet simple method which allows to predict crystal structure of particles in metallic matrices on the example of Ti–C precipitates in α-Ti. Based on ab inito energy calculations and law of mass action this method allows to compute probabilities of phase formation in dependence of temperature.

Commercially pure titanium alloys contain up to 0.3 at.% of carbon. This is enough for 214 particles/μm³ density of 40 nm particle's[1] with normalised Zener drag pressure [20] on the order of 0.18 μm^{-1} which is typical value for dispersion-hardened materials.

On the other hand, according to experimental data there are a big number of different Ti–C phases [17] and it is almost unclear what crystal structure must have Ti–C dispersed phases in α-Ti. To determine energetically favourable dispersed phases in α-Ti, some model of their formation is needed. Such process of particle formation can be very difficult, but in our case it is enough to know the initial and final state of carbon atoms. The initial state for carbon in hcp Ti is solid solution, in which carbon atoms are situated in octahedral interstitial positions [17]. The final state is

dispersed particles. If the full energy of system is lower in final state, then the process of particle formation is thermodynamically favourable. It is quite easy to obtain energy of carbon atom in octahedral site from first principles but it is impossible to calculate full energy even of very small particle in titanium matrix. Though in first assumption for large enough particles we can neglect the existence of interfaces and take into account only bulk gain using boundary periodic conditions. For example, for 40 nm Ti_2C (227)[2] particles the influence of interface will be comparable with bulk gain for interface energies more than 10 J/m². But it is well known that typical value of interface energies is about 1 J/m² and such assumption is quite reasonable. For estimation of Ti–C/hcp-Ti interface energy can be used first-principle data from Ref. [21] for TiC (225)/bcc-Ti, which is on the order of 3 J/m².

To investigate the influence of temperature on phase formation we have considered equilibrium between carbon solid solution and different Ti–C phases with the help of the law of mass action and approximation of dilute solid solution. This approximation states that average distances between solution atoms is much larger then their radii of interaction. In such conditions dispersed phases are forming independently from each other. To calculate free energies we have considered configuration entropy of C atoms in solid solution.

Summing up, using described model based on Ti–C phases we predict possible crystal structures of Ti–C particles in α-Ti at different temperatures.

3. Details of calculation

Calculations of the full energies, optimised geometries and elastic constants were performed in the framework of the density-functional theory (DFT) [30,31] within the generalised gradient approximation (GGA) using the Perdew et al. [32] functional and projected augmented wave (PAW) method [33] (ABINIT [34] and VASP code [35]). GGA provides good description of basic characteristics of Ti–C system [36]. We considered the following valence electronic states: 3s, 3p, 4s, 3d for Ti and 2s, 2p for C. The calculations were performed by using an energy cutoff of 680 eV for the plane-wave basis set and converged with respect to the k-point integration. Brillouin-zone (BZ) integrals were approximated using the special k-point sampling of Monkhorst and Pack [37]. The 14 × 14 × 8 grid was used for α-Ti. For other structures k-point grid was adopted according to the size of BZ to obtain similar densities of k-points for all unit cells. The integration over the BZ used the Methfessel–Paxton smearing method with 0.27 eV smearing width

---

[1] The estimation made for spherical particles with Ti_2C (227) structure having 67.3 Å³ volume of unit cell with 12 atoms

[2] see our results in Section 4 for bulk formation energy of Ti_2C (227) structure in hcp Ti. Number in parenthesis denote space group of the structure according to the International Union of Crystallography

Table 2
Cohesive energies and lattice parameters for different phases within DFT calculation. Cohesive energies for Ti phases were calculated w.r.t. α-Ti phase. In parentheses DFT results of Ref. [45]

Phase	E_c (meV/atom)	a (Å)	c/a
α-Ti	0 (0)	2.937 (2.947)	1.584 (1.583)
β-Ti	111 (108)	3.255 (3.261)	–
fcc-Ti	58 (58)	4.111 (4.124)	–
ω-Ti	−6 (−5)	4.575 (4.590)	0.619 (0.619)
Diamond	–	3.573	–
TiC (225)	–	4.330	–

Table 3
Elastic constants (C_{ij} in GPa) for Ti, diamond and TiC (225). The experimental values for α-Ti are measured at 4 K [46], for diamond and TiC (225) at 298 K [47].

	C_{11}	C_{12}	C_{44}	C_{33}	C_{13}
α-Ti					
GGA	176	86	45	191	76
GGA[a]	172	82	45	190	75
Exp.[b]	176	87	51	191	68
ω-Ti					
GGA	201	82	56	251	52
GGA[a]	194	81	54	245	54
β-Ti					
GGA	87	116	41	87	116
GGA[a]	95	110	42	95	110
fcc-Ti					
GGA	134	96	61	134	96
GGA[c]	136	92	61	136	92
diamond					
GGA	1053	130	566	1053	130
Exp.[d]	1076	125	576	1076	125
TiC (225)					
GGA	513	119	170	513	119
GGA-FP-LMTO [f]	470	97	167	470	97
Exp.[e]	515	106	179	515	106

[a] Ref. [45].
[b] Ref. [46].
[c] Ref. [48].
[d] Ref. [47].
[e] Ref. [49].
[f] Ref. [36].

[38]. Such choice of main parameters ensures energy convergence to 2 meV/atom. For determination of carbon energy in octahedral site, simulation cell of 48 α-Ti atoms was used. The size of the cell was enough to keep specified accuracy for energy.

The structural relaxation was stopped when all forces acting on the atoms were converged to within 3 meV/Å. Method and PAW potentials were checked by computation of lattice and elastic constants of α-Ti, β-Ti, Ω-Ti, fcc-Ti, diamond and carbide TiC (225). Results of calculation in comparison with experiment and another theoretical results are in Tables 2 and 3. The difference between DFT and experiment is less than 1% for lattice constants and 10% for elastic moduli.

The number of independent elastic constants is determined by the crystal symmetry [39]. For an orthorhombic there are nine, for trigonal material there are six, for hexagonal there are five and for cubic there are three independent elastic constants [40]. They were deduced by applying small strains to the equilibrium lattice and determining the resulting change in the total energy. For each applied strain, the total energy of the system has been calculated for nine different small distortions ($\delta = \pm 0.005n$, $n = 0-4$) used in distortion matrices. Relaxation of the internal degrees of freedom was carried out for all applied deformations. The elastic constants were computed by fitting the energies against the distortion parameter by the Taylor expansion, limited to second-order.

The components of the distortion matrices for trigonal and orthorhombic crystals can be found in Refs. [41,42] and for hexagonal and cubic crystals in Refs. [43,44].

3.1. Computation of diffraction patterns

The spots on electron diffraction patterns represent those nodes of reciprocal lattice which intersect with Ewald sphere. The radius of Ewald sphere for electron beam is very large [50] and as good approximation we replaced it by plane. The plane is given by direction in real space parallel to electron beam and normal to the plane.

The intensity of spots is proportional to $|F_{hkl}|^2$, where F_{hkl} is structure factor which was calculated by the following way:

$$F_{hkl} = \sum_i f_i exp[2\pi i(hx_i + ky_i + lz_i)],$$ (1)

where f_i is atom factor, values of which reported in Ref. [50]; h, k, l are Miller indexes for each node of reciprocal lattice; x, y, z are reduced coordinates of atoms in real space vectors of lattice. We used area of spots to show their intensity. The radius r of spot was calculated as $r = \sqrt{\pi|F_{hkl}|^2}$.

4. Results and discussion

4.1. Formation energies of Ti–C phases in α-Ti and their crystal structure at 0 K

The formation energies of phases in metallic matrices depend on underling physics. In the case of α-Ti dispersed particles are forming from solid solution at low carbon concentrations. Hence: (i) for energy origin we use the energy of carbon atom in octahedral site; and (ii) to compare energetic favourability of Ti–C phases in α-Ti we use ΔE specific formation energy on one C atom. The ΔE allows to compare systems with the same numbers of Ti and C atoms independent from phases stoichiometry.

For an arbitrary Ti–C phase the specific formation energy in α-Ti is

$$\Delta E = \frac{E(Ti_xC_y) - xE(Ti_{hcp}) - yE(C_{oct})}{y},$$ (2)

where $E(Ti_xC_y)$ is energy of simulation cell with $x + y$ atoms, $E(Ti_{hcp})$ is energy of Ti atom in α-Ti, $E(C_{oct})$ is difference between energy of 48 Ti atoms supercell with 1 carbon atom and energy of the same supercell without carbon [51]. Dividing by the number of carbon atoms allows to consider, that C_{oct} atoms always has close contact with Ti_{hcp}. Negative value of ΔE means that formation of Ti–C phase is favourable in α-Ti.

Using this equation we have calculated ΔE for fully relaxed 14 Ti–C phases from first principles. We have considered phases known from experiment [17] and some hypothetical phases consistent with diffraction data [13]. The phases only with negative ΔE are summarised in Table 4. All phases in this table, except

Table 4
Lattice constants of supercells and formation energies of Ti–C phases at 0 K.

Phase	a (Å)	c/a	ΔE (meV/atom-C)
α-Ti	17.621	1.584	–
TiC (225)	18.370	1.633	−60
Ti$_2$C (164)	18.373	1.607	−230
Ti$_2$C (166)	18.489	1.564	−360
Ti$_3$C (227)	18.301	1.633	−395
Ti$_3$C$_2$ (12)	18.401	1.623	−384
Ti$_3$C$_2$ (20)	36.748	1.630	−385
Ti$_6$C$_5$ (12)	18.414	1.632	−273

trigonal Ti$_2$C (164) can be obtained from the base cubic TiC (225) lattice by partial remove of carbon atoms with saving Ti sublattice [51]. From the Table 4 follows that maximum reduction of energy corresponds to Ti$_2$C (227) and not TiC (225). Detailed description of trigonal Ti$_2$C (166) and cubic Ti$_2$C (227) can be found in Ref. [52], monoclinic Ti$_3$C$_2$ (12) and Ti$_6$C$_5$ (12) in Ref. [53], Ti$_2$C (164) in Refs. [54,51]. The Ti$_2$C (164) can be obtained by filling half of octahedral sites in α-Ti such that there will be full and empty alternating (0001) carbon planes. The description of lattice structure of orthorhombic Ti$_3$C$_2$ (20) phase with 40 atoms in primitive cell can be found in Ref. [17]. As we know this phase was not considered earlier from first principles. One can see from Table 4 that Ti$_3$C$_2$ (20) and Ti$_3$C$_2$ (12) have similar ΔE, but there are no superstructure reflexes (1/2 1/2 1/2) for Ti$_3$C$_2$ (20) [53]. This difference in diffraction patterns can be important comparing with other phases.

Formation of phases with positive ΔE is gainless in α-Ti. For example, considered in Ref. [52] metastable tetragonal phase Ti$_2$C (123) from our calculations has ΔE = 40 meV/atom-C. The existence of trigonal Ti$_2$C (152) was proposed in Ref. [55] but later in Ref. [56] was said about impossibility of such phase on the base of cubic lattice, because of partially matched crystal lattice sites. On the other hand structure with such space group can be constructed, but our calculations showed unreality of it realisation in α-Ti with ΔE = 1.14 eV. Description of other Ti-C structures with positive ΔE: Ti$_2$C$_2$ (194), Ti$_2$C$_4$ (194), Ti$_6$C$_4$ (194) are in Ref. [51].

Hugosson et al. [57] considered TiC$_{1-m}$ phases, constructed from supercells with up to 32 atoms. Making larger supercells it is possible to obtain more structures but their consideration from first-principles will be very time consuming. We did not treat such structures in our study and leave them for further investigations with other methods.

There are works in which energies of formation of Ti-C phases was also calculated. But authors used other equation [57,52]:

$$\Delta E = \frac{E(Ti_xC_y) - xE(Ti_{hcp}) - yE(C_g)}{x + y}, \tag{3}$$

where $E(C_g)$ is energy of carbon atom in graphite structure. Also some authors used energy of C atom in vacuum instead of $E(C_g)$ [54]. Applying such equation authors [57,52] get, that TiC (225) is the lowest energy phase. But this equation is not suitable for comparison of favourability of Ti-C phases in α-Ti, because there are no graphite in CP titanium alloys. Also from dividing by $x + y$ follows that carbon atoms can interact with Ti-C structures omitting α-Ti. This is not the case for dilute solid solution in CP alloys, in which carbon atoms are immersed in α-Ti.

More descriptive explanation of Ti$_2$C (227) (and other phases with low ΔE) favourability in α-Ti can give examples in the form of chemical reactions. Consider the following reaction:

$$\text{TiC}(225) + \text{Ti}(\text{hcp}) \rightarrow \text{Ti}_2\text{C}(227) \tag{4}$$

The change of energy is $E[\text{Ti}_2\text{C} (227)] - E[\text{TiC} (225)] - E[\text{Ti} (\text{hcp})]$ = -0.335 eV. The flow of the reaction is energetically favourable. Consider other:

$$2\text{TiC}(225) \rightarrow \text{Ti}_2\text{C}(227) + \text{C}(\text{oct}). \tag{5}$$
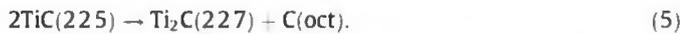
The change of energy is $E[\text{Ti}_2\text{C} (227)] + E[\text{C} (\text{oct})] - 2E[\text{TiC}]$ = -0.267 eV.

If TiC (225) is in contact with hcp titanium, the process of Ti$_2$C (227) formation is energetically favourable. Using Eq. (2) one can calculate energy changes for similar reactions, but if Ti$_2$C (227) is in contact with graphite the most likely reaction is:

$$\text{Ti}_2\text{C}(227) + \text{C}(g) \rightarrow 2\text{TiC}(225). \tag{6}$$

that are in agreement with theoretical works [57,52], but there is no graphite in technically pure titanium, and in our study we did not taken into account (6) reaction.

The difference of primitive vectors for listed Ti-C phases does not allow direct comparison of lattice parameters. To overcome this difficulty we have considered all phases in hexagonal cell with big atom basis. We have used the following lattice vectors:

$$\left(\sqrt{0.75}an, -0.5an, 0 \right); (0, an, 0); (0, 0, cn), \tag{7}$$

where a and c are parameters of hexagonal cell, n is multiplier (for Ti$_3$C$_2$ (20) n = 12; for others n = 6). For all phases hexagonal vectors were estimated finding required combinations of primitive vectors and coordinate system rotates. The a and c parameters are summarised in Table 4. The obtained primitive vectors for Ti$_3$C$_2$ (12), Ti$_6$C$_5$ (12) and Ti$_3$C$_2$ (20) phases have negligible discrepancies from (7). For these phases components of first two lattice vectors deviate by the order of 0.5% of a. That is why we provide here only a and c parameters.

4.2. Equilibrium between Ti-C precipitates and carbon solid solution

Considered Ti-C phases with negative ΔE are assumed below as prototypes for crystal structure of Ti-C precipitates. Table 4 contains energetically favourable Ti-C phases in hcp Ti at 0 K. At 0 K all carbon occupy the lowest energy state, which is Ti$_2$C (227) phase according to our data. But in real cases it is important to know temperature dependence of phase formation. As temperature rising above zero the influence of entropy contribution increasing and it must be taken into account. As a first approximation, we consider only configuration entropy of carbon solid solution, because it is the main contribution in the full entropy. We neglected the vibrational entropy, configuration entropy of C atoms in particles and configuration entropy of the whole particles in matrix.

Once temperature has become nonzero there are some probability of phase formation different from Ti$_2$C (227). Moreover Ti$_3$C$_2$ (12), Ti$_3$C$_2$ (20), Ti$_2$C (227), Ti$_2$C (166) phases have very close formation energies. This means, that at high temperatures, probabilities of precipitates formation with such structures will be very close. Also, due to low carbon concentration precipitates are forming independently from each other and there is equilibrium only between precipitates and matrix. The above-mentioned comments is true not only for Ti-C but for all analogous systems. To describe probability of phases formation in dependence from temperature, we investigated simple model, based on the law of mass action. The model is based on several approximations: (i) the solid solution of impurity atoms is dilute, (ii) secondary phases (precipitates) interact only with matrix and not with each other, (iii) kinetic factors are neglected, and (iv) only the contribution of the configuration entropy of solid solution atoms is taken into account. The detailed description of model, including deducing of solution is in Appendix. The main obtained values are $d_C(j)$ – contribution of carbon atoms in j phase (%) i.e. fraction of precipitates with j structure, where j is Ti$_3$C$_2$ (20), Ti$_2$C (227), etc. and x_C – concentration of carbon atoms in the form of solid solution (%). To describe possible crystal structure of precipitates in α-Ti we have used carbon concentration of 0.3 at.%, which is usual for Grade 4 titanium alloy. The temperature dependencies of $d_C(j)$ contributions up to temperature of polymorphic transformation in titanium (1156 K) are shown in Fig. 1.

The Ti$_3$C$_2$ (20), Ti$_2$C (227) and Ti$_2$C (166) phases prevailing in the 200–800 K temperature interval. This means there are concurrent existence mostly of three types of precipitates in such temperature interval. According to Gibbs phase rule in a two component system at fixed pressure only two phases can be in equilibrium in an interval of temperatures. But our model predict concurrent existence of four (and even more including phases with small contributions, see Fig. 1) phases. This is due to second approximation,
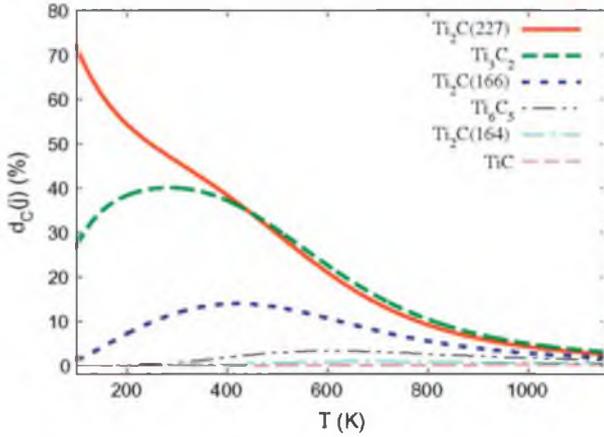
Fig. 1. Temperature dependence of carbon contributions in Ti–C structures. Total carbon concentration is 0.3 at.%.
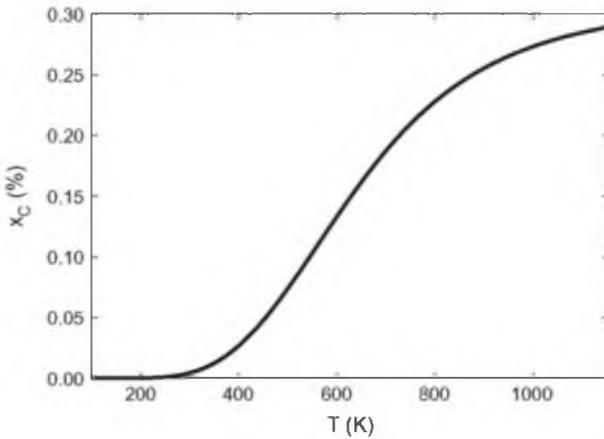
Fig. 2. Temperature dependence of carbon concentration in solid solution in units of at.%. Total carbon concentration is 0.3 at.%.

according to which there are only partial equilibrium in system; i.e there are equilibrium between phases and matrix and no equilibrium between phases. Hence all phases, except Ti_2C (227) are metastable. In real systems metastable phases can exist concurrently and independently due to kinetic factors. So our model could predict contribution of metastable phases such as Ti_3C_2 (20), Ti_2C (166) and others, see Table 4. The dependence (1) does not describe order–disorder transition, as we did not considered disordered Ti–C phases.

Another important characteristic is solubility of carbon at different temperatures. Our model allows to predict it. Fig. 2 shows temperature dependence of x_C concentration of carbon in solid solution. Due to configuration entropy contribution of carbon solid solution increases with the rise of temperature.

However, almost all phases have comparable ΔE energies and formation of precipitates will be influenced by interfaces. For example because Ti_2C (164) structure is based on hcp Ti sublattice it can have lower energy of Ti (hcp)/Ti–C interfaces in contrast to other structures based on fcc Ti lattice. Investigation of influence of interfaces on the structure of precipitates is very hard from first principles. A more suitable method is molecular dynamics, which will also allows to study sizes and morphology of Ti–C precipitates. Obtained in this study energetic characteristics, lattice and elastic constants can be used for construction of Ti–C interatomic potentials. After which the proposed model can be improved by using data from molecular dynamics.

Table 5
Theoretical values of the elastic constants (c_{ij} in GPa) of Ti–C phases.

Phase	C_{11}	C_{12}	C_{44}	C_{33}	C_{13}	C_{14}	B
Ti_2C (164)	335	59	18	253	44	−16	135
Ti_2C (166)	199	108	112	200	109	−10	139
Ti_2C (227)	203	110	117	–	–	–	141
Ti_3C_2 (20)[a]	337	83	132	331	98	–	174
TiC (225)	513	119	170	–	–	–	250

[a] For Ti_3C_2 (20) there are also: $C_{22} = 396$, $C_{23} = 84$, $C_{55} = 133$, and $C_{66} = 116$.

4.3. Elastic moduli and theoretical diffraction patterns of Ti–C phases

4.3.1. Elastic moduli
The Table 5 shows calculated elastic moduli of most favourable Ti–C phases in α-Ti. The elastic moduli provide information about the bonding characteristics between adjacent atomic planes, anisotropic character of the bonding, and structural stability. The negative value of C_{13} is allowed, because mechanical stability of lattice is determined by the Born stability criteria [58]. The Born criteria requires that all of the eigenvalues of the elastic tensor be positive. All enlisted structures satisfy this criteria. Elastic moduli have correlations with ideal shear strengths [59] and allow to make qualitative estimate of Ti–C particles influence on the strength characteristics of titanium alloys. Hence for material engineering the most appropriate structure for dispersed particles is $Ti_3C_2(20)$, as probability of formation of TiC (225) particles is low.

4.3.2. Theoretical diffraction patterns
Selected area electron diffraction (SAD), that can be performed inside a transmission electron microscope (TEM) is suitable technique for determination of crystal structure of Ti–C particles. To provide possibility of comparison of theoretical and experimental results we calculated diffraction patterns of energetically favourable Ti–C phases. Patterns for |001| (relates to [111] in cubic representation) and $|100|(|\bar{1}10|$ in cubic representation) zone axes are on Figs. 3 and 4 respectively. The side of each square in the figures in reciprocal space is 1.57 Å^{-1}. The spots in the squares are shown only for reciprocal vectors less than 0.71 Å^{-1}. Spots with diameter less than 10^{-3} Å^{-1} are not shown [3]. It can be seen from Fig. 3 that for |111| cubic zone axis Ti_2C (227) and TiC (225) has the same patterns. Also Ti_3C_2 (20) and TiC (225) has the same patterns for $|\bar{1}10|$ cubic zone axis (see Fig. 4). Such similarities can lead to erroneous interpretation of experimental data, because it can be difficult to see the same particle in several axes. Patterns of α-Ti and Ti_2C (164) for |001| hexagonal zone axis (see Fig. 3). also have similar patterns, but as α-Ti has smaller lattice parameters then Ti_2C (164) (see Table 4), it has bigger reciprocal vectors and it will be very easy experimentally to distinguish Ti_2C (164) structure even on the background of α-Ti.

4.4. Comparison with experimental data

The majority of works in Table 1 devoted to studying the effects of ordering in Ti–C system, in which authors use methods of neutron powder diffraction for determining their structure. Nevertheless superstructure peaks observed by authors are analogous to spots on diffraction patterns and it is possible to compare them. Such comparison allows to find all superstructure reflexes mentioned in Ref. [23] on theoretical diffraction patterns indicating their reliability. Two separate reflexes on diffraction patterns of type (1/2 1/2 1/2) and (1/2 1/2 −1/2) are the same in powder diffraction and that is why sets of peaks for Ti_2C (227) and Ti_2C (166)

---

[3] This diameter has no relation to the sizes of nodes in reciprocal space
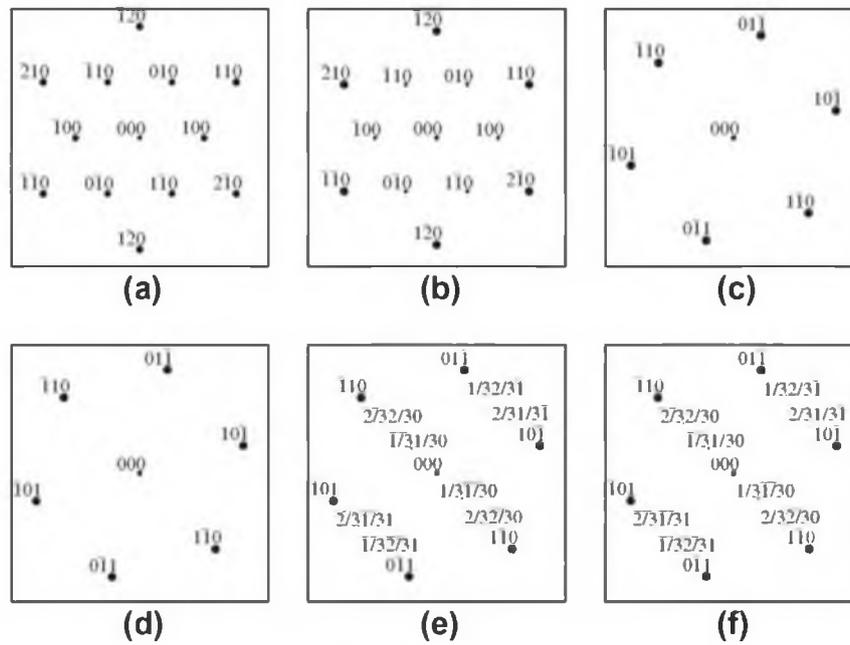
Fig. 3. Zone axis [001] ([0001]) in hexagonal representation for (a) α-Ti and (b) Ti$_2$C (164); zone axis [111] in cubic representation for (c) Ti$_2$C (166); (d) Ti$_2$C (227) and TiC (225); (e) Ti$_3$C$_2$ (20); and (f) Ti$_6$C$_5$ (20).
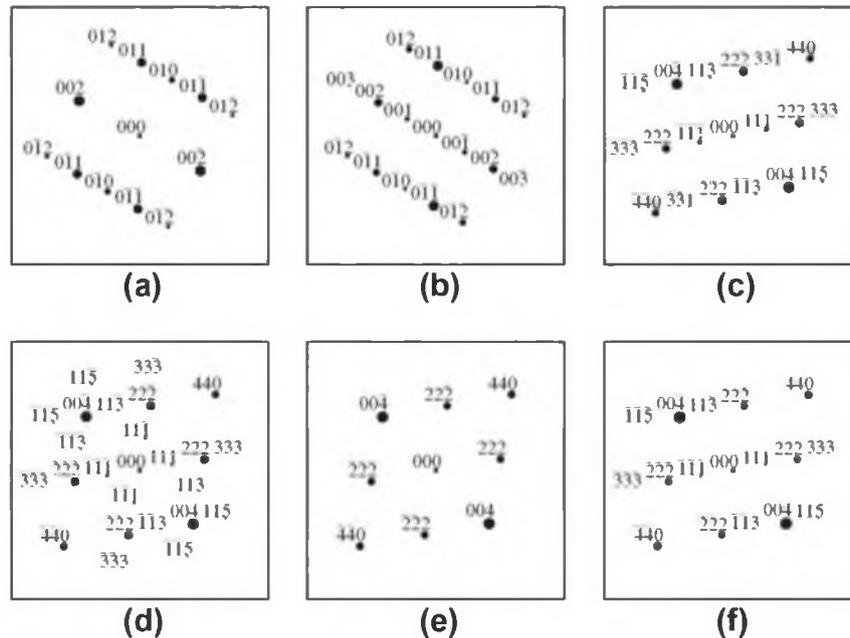
Fig. 4. Zone axis [100]([2110]) in hexagonal representation for (a) α-Ti and (b) Ti$_2$C (164); zone axis [110] in cubic representation for (c) Ti$_2$C (166); (d) Ti$_2$C (227); (e) Ti$_3$C$_2$ (20) and TiC (225); and (f) Ti$_6$C$_5$ (20). The indexes for (c–f) should be divided by 2.

are identical. Even in real SAD patterns such phases can have identical diffraction spots [60] due to superposition from several particles.

As was mentioned earlier there are no systematic experimental investigation of Ti–C structure in CP Ti. In several works [13,16,14] authors observed Ti–C particles in CP Ti, but there is very little information about structure of particles. By TEM Bushnev et al. [13] propose existence of particles with Ti$_2$C stoichiometry (they propose a model of lattice which is consistent with Ti$_2$C (164) structure) stable up to 823 K. Ivanov et al. [14] determined

particles with TiC (225) structure by selected diffraction area in TEM in [110] zone axis. Therefore they could observe particles with Ti$_3$C$_2$ (20) structure as their patterns in this zone are equal.

Also there are several works mainly on Ti–TiC composites, in which structure of dispersed Ti–C phases were established. Ranganath et al. [61] prepare titanium–titanium carbide composites by a combustion-assisted synthesis route. They showed from thermochemical considerations that formation of Ti$_2$C structure in the presence of excess titanium is more favourable than TiC (225) and proved this by electron probe microanalysis. They claimed that the

reaction (4) is more probable in present of additional moles of titanium, which is in agreement with our first-principle results. The exact value of profit is 0.335 eV at 0 K.

In Ref. [25] formation of phase with Ti_2C stoichiometry in the interface between TiC particles and Ti-6%Al-4%V (Grade-5 $\alpha + \beta$) matrix was observed by means of neutron diffraction and low voltage field emission gun scanning electron microscopy. Moreover, for the composite material processed at 1773 K, within half an hour of sintering, the complete transformation of TiC particles to Ti_2C was observed. Though V and Al can influence this transformation, more probably that interaction of TiC with Ti (hcp) lead to formation of more energetically favourable in such conditions particles with Ti_2C structure.

Vallauri et al. [62] suppose that in spite of all these observations, the existence of a Ti_2C phase in the Ti-C system remains questionable, primarily because $TiC_{(1-x)}$ can easily pick up oxygen to form titanium oxycarbides of various compositions. Such statement need additional checking.

Finally there is recent study of prepared by reactive arc-melting method Ti-TiC composites in which microstructural changes in the TiC particles by the combined effect of N and Fe elements were studied [60]. By means of SAD authors identify Ti_2C structures in TiC (225) particles by clear spots in Ti alloy with 3% of Fe and by very diffused spots in Ti alloys: Ti with 3% Fe and 3% N; Ti with 10% Fe; (all in at.%). Interaction of TiC (225) with α-Ti leads to Ti_2C formation which is in agreement with our result. Authors could not determine symmetry group of Ti_2C structure because their diffraction patterns are indistinguishable. But our calculation showed that Ti_2C (227) is more favourable then trigonal Ti_2C (166) by 35 meV/atom-C. Our theoretical diffraction patterns for Ti_2C (227) are in good agreement with experimental one [60] for spots positions and also for spot sizes.

Some explanation can be given why several authors [63,6,15, 64,65] did not found Ti-C particles in CP-Ti. Observation of coherent particles with transmission electron microscopy (TEM) is possible due to strain contrast. At the same time if particle is situated on the grain boundary, it became invisible on the background of grain boundary strain contrast with the use of TEM.

5. Conclusions

We have presented new approach for calculating specific formation energies of dispersed phases in matrix material accounting underling physics. We have used PAW GGA plane-waved method to calculate specific formation energies of Ti-C phases in α-titanium and found that the most favourable phase at 0 K is Ti_2C (227). This surprising result is due to the choice of energy reference, which is the energy of carbon atom in octahedral site, the case for commercially pure α-Ti alloys. Further we have investigated model, based on specific formation energies and the law of mass action, to predict probabilities of Ti-C phases formation in dependence of temperature. According to the model, which consider configuration entropy of carbon solid solution, there are concurrent existence of mostly Ti_3C_2 (20), Ti_2C (227) and Ti_2C (166) phases in 200-800 K temperature interval. The discovered phases can serve as prototypes for crystal structure of dispersed particles in α-Ti alloys. Rough estimates have shown that for large enough particles (more than 40 nm) the influence of interfaces on bulk structure of particles can be neglected. Such methodology of consideration of Ti-C phases in hcp titanium is made for the first time and can used for other impurities in many metallic matrices.

Calculation of elastic moduli have shown that carbon richer phases have higher moduli. Hence for material engineering the most appropriate structure for dispersed particles is Ti_3C_2 (20) as elastic moduli have correlations with strengths characteristic.

Finally, we have computed diffraction patterns of favourable Ti-C phases, which can be used in experimental determination of Ti-C particles in α-Ti alloys by selected area diffraction in TEM.

The obtained results about Ti-C particles structure can be used for further investigation of thermostability of nanostructured titanium.

Appendix A. Equations of phases equilibrium

To consider equilibrium between n Ti-C structures with carbon solid solution we used n following reactions:

$$Ti_x(hcp) + yC(oct) \rightarrow Ti_mC(j), \tag{A.1}$$

where $m = \frac{x}{y}$. As atoms of Ti (hcp) are bonded, we can treat them like agglomerates with x atoms. The set of Eq. (A.1) is correct until Ti-C particles are in contact with hcp titanium. Because carbon atoms in dilute solid solution are isolated from each other we treated them separately. Introduced in Section 4 the ΔE parameter can be defined as energy change due to imaginative cluster Ti_mC (j) formation from one carbon atom and m hcp Ti atoms. It is obvious that Ti-C particles consists of more then thousands of atoms and there are no problems with fractional numbers of atoms, but for mathematical handling it is convenient to use Ti_mC (j). For every Eq. (A.1) write down the law of mass action [19]:

$$K(j) = \frac{a[Ti_mC(j)]}{a[Ti_m(hcp)]a[C(oct)]}, \tag{A.2}$$

where a is activity of species. By definition $a = \gamma c$, where c is concentration of species and γ is coefficient of activity. To find γ we use definition of chemical potential:

$$\mu = \mu_0 + k_B T \ln(\gamma c), \tag{A.3}$$

where μ_0 is chemical potential of reference state, k_B is Boltzman constant. Because of small carbon concentrations, solid solution can be treated as regular, where $\gamma = 1$ [19]. For $Ti_m(hcp)$ and Ti_mC (j) the energy reference is chosen such that at $c = 1$ must be fulfilled $\mu = \mu_0$. Using (A.3) and the fact that coefficient of activity does not depend from concentration get $\gamma = 1$. Because the coefficient of activity for all cases is equal to one, we can write the law of mass action for concentrations:

$$K(j) = \frac{[Ti_mC(j)]}{[Ti_m(hcp)][C(oct)]}. \tag{A.4}$$

The generation rate constant of Ti_mC (j) cluster is:

$$K(j) = A(j,T)e^{-\Delta G\beta}, \tag{A.5}$$

where $\beta = 1/k_B T$, $\Delta G = \Delta E - T\Delta S$ is change of Gibbs free energy at zero pressure and $A(j,T)$ is pre-exponential factor. We take $A(j,T) = 1$ for all structures and temperatures.

Next, find dependence of C and Ti atoms contributions in Ti-C structures from temperature. Introduce symbols: n is the number of carbon states in studied system except carbon in octahedral sites, N is the number of Ti and C atoms. N_C is the number of C atoms, N_{Ti} is the number of Ti atoms, $N_C(oct)$ is the number C atoms in octahedral sites, $N_{Ti}(hcp)$ is the number of Ti atoms in hcp lattice, $N_C(j)$ is the number C atoms in state j, $N_{Ti}(j)$ is the number of Ti atoms in state j.

The numbers of atoms are related as follows:

$$\begin{cases} N_C(\text{oct}) + \sum_j N_C(j) = N_C \\ N_{Ti}(\text{hcp}) + \sum_j N_{Ti}(j) = N_{Ti} \end{cases} \tag{A.6}$$

To obtain relationships between concentrations we divided (A.6) by N. Denote concentrations: $[C(\text{oct})] = \frac{N_C(\text{oct})}{N}$ is concentration of C atoms in octahedral sites, $[Ti(\text{hcp})] = \frac{N_{Ti}(\text{hcp})}{N}$ is concentration of Ti atoms in hcp lattice, $[Ti_m(\text{hcp})] = \frac{Ti(\text{hcp})}{m}$ is concentration of Ti clusters in hcp lattice, $x_0 = \frac{N_C}{N}$ is total concentration of carbon atoms (0.3 at.% for Grade 4 alloy), $[Ti_mC(j)] = \frac{N_C(j)}{N} = \frac{N_{Ti}(j)}{m(j)N}$ is concentration of $Ti_mC(j)$ clusters. Using the law of mass action for concentrations (A.4) derive n equations:

$$[Ti_mC(j)] = \frac{K(j)}{m(j)}[Ti(\text{hcp})][C(\text{oct})]. \tag{A.7}$$

Obtained system of Eqs. (A.6) and (A.7) was solved self-consistently in the range of temperatures from 100 K up to temperature of allotropic transformation of α-titanium to β-titanium. Additional self-consistency loop was used to resolve dependence of the equilibrium constant from entropy.

The equation for change of configuration entropy related to transition of one carbon atom from solid solution to ordered structure is equal to entropy of formation of one vacancy. Skipping some computations we have for entropy change:

$$\Delta S = -k_B\left(1 + \frac{[C(\text{oct})]}{[Ti(\text{hcp})]} - \ln\frac{[C(\text{oct})]}{[Ti(\text{hcp})]}\right). \tag{A.8}$$

Here we assumed that N_{Ti} is much bigger than N_C and neglected entropy of carbon atom in Ti-C cluster, entropy of Ti-C cluster in Ti matrix and vibrational entropy.

It is convenient to represent results in the form of contributions of carbon atoms in different structures and carbon concentration in solid solution. Define corresponding quantities: $x_C = \frac{N_C(\text{oct})}{N_C(\text{oct}) + N_{Ti}(\text{hcp})}$ is carbon concentration in solid solution. Multiplying and dividing by N we have: $x_C = \frac{[C(\text{oct})]}{[C(\text{oct})] + [Ti(\text{hcp})]}$. The contributions of Ti and C atoms in j structure defined as follows: $d_{Ti}(j) = \frac{N_{Ti}(j)N}{N_{Ti}(\text{hcp})N} = \frac{m(j)[Ti_mC(j)]}{1 - x_0}$, $d_C(j) = \frac{N_C(j)N}{N_C(\text{oct})N} = \frac{[Ti_mC(j)]}{x_0}$.

References

[1] M.A. Miodownik, Scripta Materialia 54 (2006) 993–997.
[2] Yu. R. Kolobov, R.Z. Valiev, Grain Boundary Diffusion and Properties of Nanostructured Materials, Cambridge International Science Publishing, 2007.
[3] Yu.R. Kolobov, O.A. Kashin, E.E. Sagymbaev, E.F. Dudarev, L.S. Bushnev, G.P. Grabovetskaya, G.P. Pochivalova, N.V. Girsova, V.V. Stolarov, Russian Physics Journal 43 (2000) 71–78.
[4] Yu.R. Kolobov, Nanotechnologies in Russia 4 (2010) 758–775.
[5] M.B. Ivanov, Yu. R. Kolobov, E.V. Golosov, I.N. Kuz'menko, V.P. Veinov, D.A. Nechaenko, E.S. Kungurtsev, Nanotechnologies in Russia 6 (2011) 370–378.
[6] V.V. Stolyarov, Y. Zhu, I.V. Alexandrov, T.C. Lowe, R.Z. Valiev, Materials Science and Engineering: A 299 (2001) 59–67.
[7] M. Hoseini, M. Hamid Pourian, F. Bridier, H. Vali, J.A. Szpunar, P. Bocher, Materials Science and Engineering: A 532 (2012) 58–63.
[8] Y.R. Kolobov, A.G. Lipnitskii, M.B. Ivanov, I.V. Nelasov, S.S. Manokhin, Russian Physics Journal 54 (2011) 918–936.
[9] J. Driver, Scripta Materialia 51 (2004) 819–823.
[10] V.Y. Novikov, Materials Letters 62 (2008) 3748–3750.
[11] C. Xu, M. Furukawa, Z. Horita, T.G. Langdon, Acta Materialia 51 (2003) 6139–6149.
[12] D. Handtrack, B. Sauer, C. Kieback, Journal of Materials Science (2008) 671–679.
[13] L.S. Bushnev, L.V. Chernova, N.V. Girsova, Fizika Metallov i Metallovedenie 34 (2001) 44–51.
[14] M. Ivanov, S. Manokhin, D. Nechaenko, Russian Physics 54 (2011) 1–7.
[15] I. Semenova, G. Salimgareeva, G. Da Costa, Advanced Engineering Materials 12 (2010) 803–807.
[16] F. Despang, A. Bernhardt, A. Lode, T. Hanke, D. Handtrack, B. Kieback, M. Gelinsky, Acta Biomaterialia 6 (2010) 1006–1013.
[17] A.I. Gusev, A.A. Rempel, A.J. Magerl, Disorder and Order in Strongly Nonstoichiometric Compounds: Transition Metal Carbides, Nitrides, and Oxides, vol. 47, Springer-Verlag, 2001.
[18] D.A. Andersson, P.A. Korzhavyi, B. Johansson, Calphad 32 (2008) 543–565.
[19] A.B. Kudryavtsev, R.F. Jameson, W. Linert, The Law of Mass Action, Springer Verlag, 2001.
[20] A.R. Eivani, S. Valipour, H. Ahmed, J. Zhou, J. Duszczyk, Metallurgical and Materials Transactions A 42 (2010) 1109–1116.
[21] L. Liu, S. WANG, H. YE, Jouranl of Material Science and Technology 19 (2003) 541.
[22] H. Goretzki, Physica Status Solidi (B) 20 (1967) K141–K143.
[23] V. Lipatnikov, L. Zueva, A. Gusev, A. Kottar, Physics of the Solid State 40 (1998) 1211–1218.
[24] M.Y. Tashmetov, V.T. Em, C.H. Lee, H.S. Shim, Y.N. Choi, J.S. Lee, Physica B: Condensed Matter 311 (2002) 318–325.
[25] P. Wanjara, R.A.L. Drew, J. Root, S. Yue, Acta Materialia 48 (2000) 1443–1450.
[26] N. Lorenzelli, R. Caudron, J.P. Landesman, C.H. de Novion, Solid State Communications 59 (1986) 765–769.
[27] S. Tsurekawa, H. Yoshinaga, Journal of the Japan Institute 56 (1992) 133–141.
[28] V.T. Em, M. Yu. Tashmetov, Physica Status Solidi (B) 198 (1996) 571–575.
[29] V. Moisy-Maurice, Structure atomique des carbures non-stoechiometriques de metaux de transition., Rapport CEA-R-5127., Commissariat a l'Energie Atomique. Gif-sur-Yvette, France, 1981.
[30] P. Hohenberg, W. Kohn, Physical Review 136 (1964) B864–B871.
[31] W. Kohn, L.J. Sham, Physical Review 140 (1965) A1133–A1138.
[32] J.P. Perdew, K. Burke, Y. Wang, Physical Review B 54 (1996) 16533–16539.
[33] P.E. Blochl, O. Jepsen, O.K. Andersen, Physical Review B 49 (1994) 16223–16233.
[34] X. Gonze, J.M. Beuken, R. Caracas, F. Detraux, M. Fuchs, G.M. Rignanese, L. Sindic, M. Verstraete, G. Zerah, F. Jollet, M. Torrent, A. Roy, M. Mikami, P. Ghosez, J.Y. Raty, D.C. Allan, Computational Materials Science 25 (2002) 478–492.
[35] G. Kresse, J. Hafner, Physical Review B 47 (1993) 558.
[36] R. Ahuja, O. Eriksson, J.M. Wills, B. Johansson, Physical Review B 53 (1996) 3072–3079.
[37] H.J. Monkhorst, J.D. Pack, Physical Review B 13 (1976) 5188–5192.
[38] M. Methfessel, A.T. Paxton, Physical Review B 40 (1989) 3616–3621.
[39] J.F. Nye, Physical properties of crystals: their representation by tensors and matrices, Clarendon, Oxford, 1957.
[40] D.C. Wallace, Thermodynamics of Crystals, in: Duane C. Wallace (Ed.), Wiley New York, 1972.
[41] J. Zhao, J.M. Winey, Y.M. Gupta, Physical Review B 75 (2007) 094105.
[42] M. Mattesini, S.F. Matar, Physical Review B 65 (2002) 075110.
[43] L. Fast, J.M. Wills, B. Johansson, O. Eriksson, Physical Review B 51 (1995) 17431–17438.
[44] P. Söderlind, O. Eriksson, J.M. Wills, A.M. Boring, Physical Review B 48 (1993) 5844–5851.
[45] R.G. Hennig, T.J. Lenosky, D.R. Trinkle, S.P. Rudin, J.W. Wilkins, Physical Review B 78 (2008) 054121.
[46] E.S. Fisher, C.J. Renken, Physical Review 135 (1964) A482–A494.
[47] H.J. McSkimin, W.L. Bond, Physical Review 105 (1957) 116–121.
[48] A. Aguayo, G. Murrieta, R. de Coss, Physical Review B 65 (2002) 092106.
[49] R. Chang, L.J. Graham, Journal of Applied Physics 37 (1966) 3778–3783.
[50] B. Fultz, J.M. Howe, Transmission Electron Microscopy and Diffractometry of Materials, Springer Verlag, 2007.
[51] A.G. Lipnitskii, D.A. Aksenov, Y.R. Kolobov, Russian Physics Journal 52 (2009) 1047–1051.
[52] R. Eibler, Journal of Physics: Condensed Matter 19 (2007) 196226.
[53] P.A. Korzhavyi, L.V. Pourovskii, H.W. Hugosson, A.V. Ruban, B. Johansson, Physical Review Letters 88 (2001) 015505.
[54] D.L. Price, B.R. Cooper, Physical Review B 39 (1989) 4945.
[55] B.V. Khaenko, V.V. Kukol', Kristallografiya 34 (1989) 1513.
[56] V. Lipatnikov, A. Gusev, JETP Letters 69 (1999) 669–675.
[57] H.k. Hugosson, P. Korzhavyi, U. Jansson, B. Johansson, O. Eriksson, Physical Review B 63 (2001) 1–8.
[58] M. Born, K. Huang, Dynamical Theory of Crystal Lattices, Oxford University Press, 1954.
[59] W. Luo, D. Roundy, M.L. Cohen, J.W. Morris, Physical Review B 66 (2002) 094110.
[60] G. Amirthan, K. Nakao, M. Balasubramanian, H. Tsuda, S. Mori, Journal of Materials Science 46 (2010) 1103–1109.
[61] S. Ranganath, J. Subrahmanyam, Metallurgical and Materials Transactions A 27 (1996) 237–240.
[62] D. Vallauri, I. Atiasadrian, A. Chrysanthou, Journal of the European Ceramic Society 28 (2008) 1697–1713.
[63] A. Popov, I. Pyshmintsev, S. Demakov, Scripta Materialia 37 (1997) 1089–1094.
[64] R.Z. Valiev, Journal of Materials 3 (2010) 407–410.
[65] M. Greger, Manufacturing Engineering 40 (2010) 33–40.